Volume 11 | Number 35 | 21 September 2015 | Pages 6907–7068

Soft Matter

www.softmatter.org

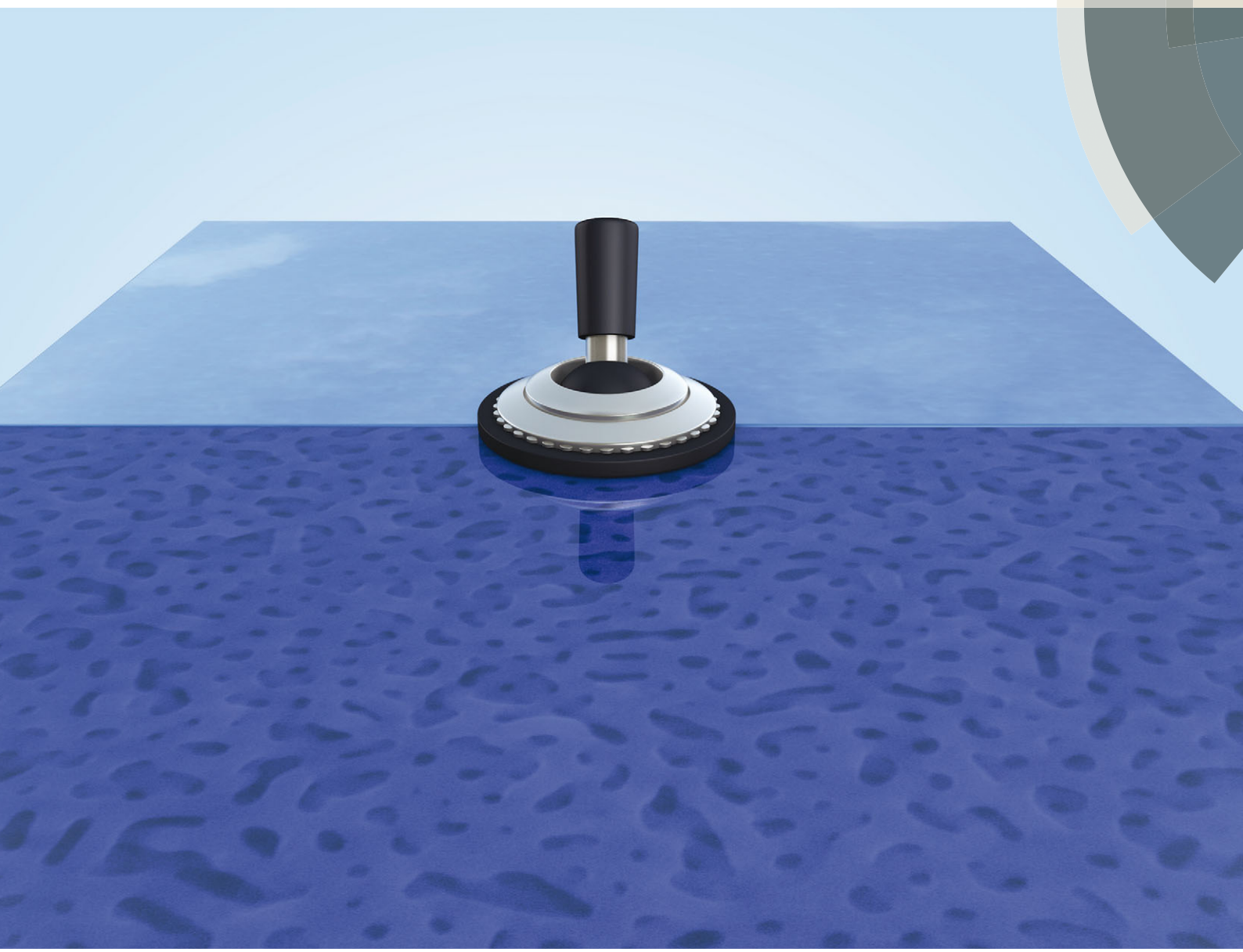

ISSN 1744-683X

ROYAL SOCIETY OF CHEMISTRY

PAPER
Nina Yan and Yong Wang
Reversible switch between the nanoporous and the nonporous state of amphiphilic block copolymer films regulated by selective swelling

Soft Matter

PAPER

View Article Online
View Journal | View Issue

Cite this: *Soft Matter*, 2015, 11, 6927

Reversible switch between the nanoporous and the nonporous state of amphiphilic block copolymer films regulated by selective swelling†

Nina Yan and Yong Wang*

Received 8th June 2015,
Accepted 17th July 2015

DOI: 10.1039/c5sm01405k

www.rsc.org/softmatter

Switchable nanoporous films, which can repeatedly alternate their porosities, are of great interest in a diversity of fields. Currently these intelligent materials are mostly based on polyelectrolytes and their porosities can change only in relatively narrow ranges, typically under wet conditions, severely limiting their applications. Here we develop a new system, which is capable of reversibly switching between a highly porous state and a nonporous state dozens of times regulated simply by exposure to selective solvents. In this system nanopores are created or reversibly eliminated in films of a block copolymer, polystyrene-*block*-poly(2-vinyl pyridine) (PS-*b*-P2VP), by exposing the films to P2VP-selective or PS-selective solvents, respectively. The mechanism of the switch is based on the selective swelling of the constituent blocks in corresponding solvents, which is a nondestructive and easily controllable process enabling the repeatable and ample switch between the open and the closed state. Systematic microscopic and ellipsometric characterization methods are performed to elucidate the pore-closing course induced by nonsolvents and the cycling between the pore-open and the pore-closed state up to 20 times. The affinity of the solvent for PS blocks is found to play a dominating role in determining the pore-closing process and the porosities of the pore-open films increase with the cycling numbers as a result of loose packing conditions of the polymer chains. We finally demonstrate the potential applications of these films as intelligent antireflection coatings and drug carriers.

1. Introduction

Switchable nanoporous materials are able to reversibly alternate their porosities between the open and the closed state triggered by external stimuli such as pH, redox potentials, and solvents. They find interesting applications in a diversity of fields from intelligent optical coatings[1,2] and gating membranes[3,4] to biomedicines.[5,6] Most of these "smart" systems display their switchability in the wet state realized by the conformational change of the polymer chains anchored onto the pore walls in response to environmental stimuli. For example, porous membranes with their pore walls grafted with weak polyelectrolytes, *i.e.* poly(acrylic acid) (PAA), poly(vinyl pyridine), poly(*N*-isopropylacrylamide) (PNIPAM), exhibit pH or thermal sensitive permeability due to the change in the effective pore size determined by the conformation of the polyelectrolytes in water.[7–9] However, upon drying the polyelectrolyte chains initially covering the pores in aqueous environments collapse, leading to a fixed porosity and the loss of the switchability in pore sizes. This switchability only valid in the wet state severely limits its applications in many occasions.

There are very few approaches to nanoporous materials with switched pores preserved in the dry state, and they are predominantly based on the ion/electron-governed chain conformation of polyelectrolytes including poly(ionic liquids).[1,3,10,11] Rubner *et al.* switched the multilayered films of two oppositely charged polyelectrolytes produced *via* the layer-by-layer technique between a more porous state and a denser state by exposing the films to water with different pH values which determined the degree of the protonation of the carboxylic acids in the PAA chains. The more porous and denser morphologies of the films were well preserved after taking the films from the water bath and these films were employed as erasable antireflection coatings.[1] In these polyelectrolyte-based switchable nanoporous materials, the switch can be readily triggered by the moderate pH change between 1.8 and 5.5, which renders appealing ease in the operation of the switch on one hand but may also result in adverse porosity shifts and morphology changes with variations in environmental pH on the other hand. Therefore, for the sake of available morphologies, materials' properties, and broader

State Key Laboratory of Materials-Oriented Chemical Engineering, College of Chemical Engineering, Nanjing Tech University, Nanjing 210009, Jiangsu, P. R. China. E-mail: yongwang@njtech.edu.cn; Fax: +86-25-8317 2292

† Electronic supplementary information (ESI) available. See DOI: 10.1039/c5sm01405k

applications, switchable nanoporous structures made from other materials, which should helpfully supplement the presently predominantly studied polyelectrolyte systems, are highly demanded.

The repeated switches between the open and the closed state of a material rely on nondestructive mechanisms both for pore formation and pore elimination. We demonstrated that swelling with a selective solvent is an effective method to create nanopores in materials composed of amphiphilic block copolymers.[12–15] In addition, our recent work revealed that the opened micellar cores of the block copolymers could be closed by exposure to solvents selective to the blocks composed of the micellar coronae.[16] Therefore, selective swelling of block copolymers may provide a new avenue to switchable nanoporous materials. A few studies reported efforts towards thin films with reversibly tunable porosities based on block copolymers. Kim and coworkers demonstrated that cylindrical pores in annealed thin films of polystyrene-*block*-poly(methyl methacrylate) (PS-*b*-PMMA) formed by solvent swelling in acetic acid could be transformed into a more closed porosity with discrete or partially interconnected pores by thermal annealing at 155 °C for 2 days under vacuum.[17] Han *et al.* realized the transition from a porous structure composed of loosely packed micelles of polystyrene-*block*-poly(4-vinyl pyridine) (PS-*b*-P4VP) induced by swelling in acetic acid to a denser structure with circular pores having the diameter of 30–80 nm by annealing in PS-selective solvents at −7 °C for 2 h.[2] Both studies showed that the switch between a more porous morphology and a denser morphology can be repeated three or four times. No work exists until now for switches between a highly porous state and a closed state. In addition, tedious and complex measures to trigger the switches should be avoided and the open and the closed state should be induced by easy and distinct methods. Moreover, ideally the materials are expected to be robust enough to allow switches many times, for example, several tens of times, for long-term applications.

In this work, we develop a robust intelligent system capable of switching between a highly porous state and a nonporous state dozens of times simply regulated by exposure to selective solvents. We produce nanoporous PS-*b*-P2VP films with varying thicknesses by ethanol swelling and then investigate the morphology evolvement from nanoporous to nonporous by exposure to nonpolar solvents having varying affinities for PS blocks. The films are further swelling-treated in ethanol to regenerate the pores. Such an alternative treatment in nonpolar solvents and ethanol is repeated dozens of times and the morphology changes with repeated times are studied in detail. We then exploit the applications of these films as intelligent antireflection coatings and carriers for drug delivery allowed by the smart function of repeatedly switching between the open and the closed state of the relatively thick films.

2. Experimental section

Materials

Asymmetric diblock copolymers of polystyrene-*block*-poly(2-vinyl pyridine) (PS-*b*-P2VP and hereafter denoted as S2VP, M_n^{PS} = 50 000 g mol^{-1}, M_n^{P2VP} = 16 500 g mol^{-1}) with a polydispersity of 1.09 were purchased from Polymer Source Inc., Canada. All chemicals including ethanol, chloroform, cyclohexane (CH), and *n*-pentane (*n*PT) were supplied by local manufacturers in the analytical grade and used as received. Bovine serum albumin (BSA, 67 kDa) was obtained from Aladdin and used without further purification. Phosphate buffer saline (PBS) solutions were prepared by mixing different amounts of NaCl, KCl, $Na_2HPO_4{\cdot}12H_2O$, and KH_2PO_4 in deionized water and adjusting them to desired pH values with NaOH or HCl solutions.

Switching S2VP films between the nanoporous and the nonporous state

S2VP solutions with a concentration of 3 wt% were obtained by dissolving the block copolymers in chloroform and then filtered through 0.22 μm polytetrafluoroethylene (PTFE) syringe filters three times. The S2VP solutions were then spincoated (2000 rpm, 30 s) on cleaned silicon wafers to obtain dense S2VP films, which were then immersed in ethanol at 70 °C for 1 h to generate pores. The ethanol-treated films in the pore-open state were then immersed in CH or *n*PT at a preset temperature for various durations to perform the pore closing process. After withdrawing from the solvent, the films were allowed to stand in air at room temperature for *ca.* 10 min to evaporate the remaining solvent. To explore the cycling between opening and closing of the film, the as-coated film was alternatively immersed in ethanol at 70 °C for 1 h and in CH at 30 °C for 5 min up to 20 times.

Antireflection coatings on glass slides

Antireflection coatings were deposited on K9 glass slides and a S2VP solution with a concentration of 0.8 wt% was used to obtain thicknesses appropriate for antireflection. The S2VP-coated glass slides were alternatively immersed in ethanol at 70 °C for 1 h and in CH at 30 °C for 5 min to induce the pore-open state and the pore-closed state, respectively. The transmittance of the glass slides in the wavelength range of 400–2000 nm was measured using a UV-vis-NIR spectrophotometer (Lambda 950, Perkin Elmer).

The uptake and release of proteins

To prepare thicker films for use in drug delivery, the solution (3 wt%, 50 μL) was dropped onto the silicon substrate. After the evaporation of the solvent, the as-prepared films were vacuum dried in an oven at 70 °C for 2 h. Afterwards, the coated substrates were immersed in ethanol at 70 °C for 18 h and the porous films with a thickness of approximately 15 μm were acquired. To load proteins into the porous film, we dropped several droplets of the BSA solution with a concentration of 20 mg mL^{-1} onto a glass substrate and then placed the 15 μm-thick porous film on the top of the solution immediately. Several seconds later, the pores of the film were filled with the BSA solution through the capillary force. Afterwards, the remaining liquid was removed from the film by spincoating at 5000 rpm for 10 s. The release experiment was performed in PBS (pH 7.4) at 25 °C and the

concentrations of the released samples at defined time periods were measured using a spectrophotometer (NanoDrop 2000C, Thermo) at a wavelength of 280 nm.

Characterization

The thicknesses of the films at different stages were determined using a spectroscopic ellipsometer (Complete EASE M-2000U, J.A. Woollam) with an incidence angle of 65°. The surface and internal morphologies of the films under different conditions were examined using a field emission scanning electron microscope (FESEM, Hitachi S-4800). Prior to examination, the samples were vacuum coated with a platinum–palladium alloy for a few seconds. A contact angle goniometer (Dropmeter A-100, Maist) was used to quantitatively determine the static water contact angles (WCAs) of the films. The reported values were an average of not less than three measurements at different positions for every sample.

3. Results and discussion

3.1 Morphology change during the pore closing process

We spincoated the 3 wt% S2VP solutions on cleaned silicon wafers and obtained nonporous films with a thickness of 440 ± 15 nm as measured by ellipsometry. The as-coated, nonporous films were then immersed in ethanol at 70 °C for 1 h to create pores inside the films following the selective swelling-induced pore generation mechanism.[18] As shown in Fig. 1a, swelling treatment in hot ethanol converted the original dense films to highly porous films featured as interconnected nanopores. The films exhibit a thickness of 1086 ± 36 nm which is much larger than that of the pristine as-coated films due to the presence of a large number of nanopores. As the pore-opening process induced by ethanol swelling has been extensively studied and is well understood,[13,18–22] detailed research is focused on the pore-closing process trigged by nonpolar solvents in the present work.

We immersed the porous films into different nonpolar solvents and investigated their morphological evolvement. Opposite to the swelling process using ethanol, which is a selective solvent to the P2VP blocks, nonpolar solvents, which are more affinitive to the PS blocks, should be employed to drive the closing of the opened pores. The solvent selectivity to a block copolymer means different affinities of a solvent for the constituent blocks, which can be estimated by comparing their polymer–solvent interaction parameters, $\chi_{\text{Polymer–Solvent}}$.[13] A lower $\chi_{\text{Polymer–Solvent}}$ indicates better solubility of the polymer in the solvent. If $\chi_{\text{Polymer–Solvent}} < 0.5$, the solvent is considered as a good solvent to the polymer and the solvent is regarded as a poor solvent or nonsolvent to the polymer in the case of $\chi_{\text{Polymer–Solvent}} > 0.5$.[23] $\chi_{\text{Polymer–Solvent}}$ can be calculated using the following equation:[24]

$$\chi_{\text{Polymer–Solvent}} = V_{\text{Solvent}}(\delta_{\text{Solvent}} - \delta_{\text{Polymer}})^2/RT + 0.34 \quad (1)$$

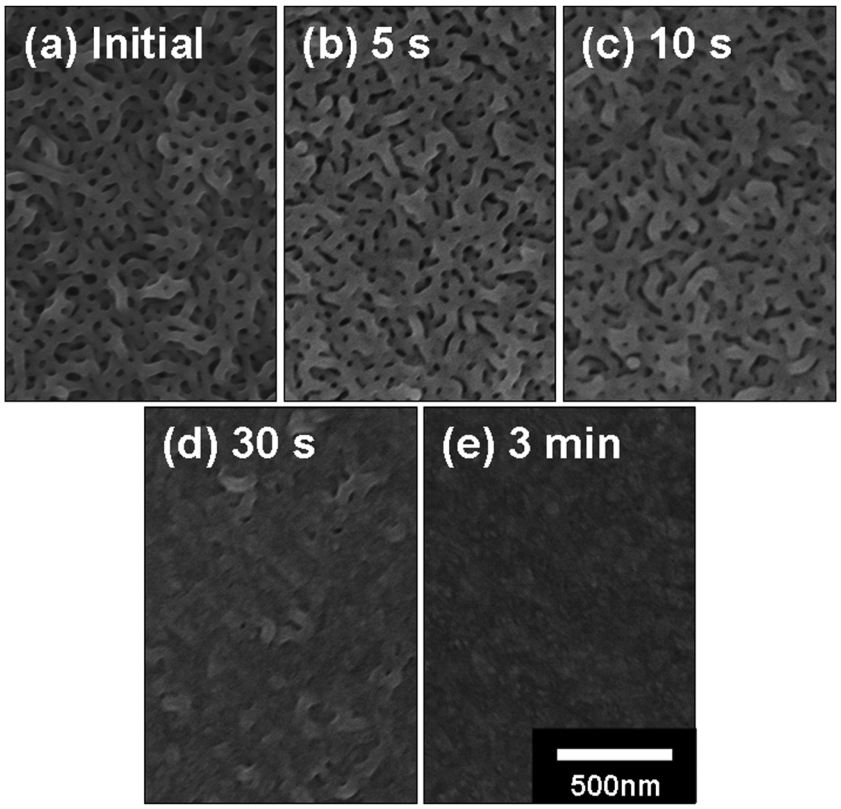

Fig. 1 The surface SEM images of the porous S2VP films produced by ethanol swelling before (a) and after exposure to CH at 22 °C for 5 s (b), 10 s (c), 30 s (d), and 3 min (e). All the SEM images have the same magnification and the scale bar is shown in (e).

where $V_{Solvent}$ is the molar volume of the solvent, $\delta_{Solvent}$ and $\delta_{Polymer}$ are the solubility parameters of the solvent and the polymer, respectively, and R and T represent the gas constant and the Kelvin temperature, respectively. The polymer–solvent interaction parameters involved in this work were calculated here by considering that δ_{PS} = 18.6 $MPa^{1/2}$ and δ_{P2VP} = 20.6 $MPa^{1/2}$,[25] and the results are listed in Table 1. As χ_{PS-CH} and $\chi_{P2VP-CH}$ are 0.48 and 0.98, respectively at the temperature of 22 °C, CH should be considered as a PS-selective solvent showing stronger affinity for PS than for P2VP.

CH was first used to close the pores in the porous S2VP films as it exhibits a moderate selectivity to PS than to P2VP. When immersed in CH, the porous films can progressively recover to their initial nonporous morphologies. Fig. 1b–e display the surface morphologies of the films being treated in CH at 22 °C for different durations. A short exposure to CH, for instance, 5 s or 10 s, did not evidently change the morphology of the film except for slightly narrowed pore sizes and the film remained highly porous (Fig. 1b and c *vs.* Fig. 1a). By contrast, most of the pores disappeared and only a few smaller pores were left after an extended exposure to CH for 30 s (Fig. 1d). For further prolonged exposure duration of 3 min, the pores were completely invisible and the film obtained a dense and smooth surface (Fig. 1e). We observed no further change in the surface morphology even for longer CH exposure up to 2 h, suggesting that the pores of the films can be thoroughly closed at 22 °C in CH for only 3 min.

It is known that the S2VP film after ethanol swelling possesses a core/shell structure with the PS skeleton wrapped by the P2VP blocks as a result of selective enrichment of P2VP blocks on the surface. Upon exposure of the porous S2VP film to CH, the penetration of CH into the film mainly contains three steps. The first step is the filling of CH into the film pores due to the capillary force which occurs very fast as these pores are interconnected to each other and fully accessible to the solvent. The second step is the diffusion of CH into the P2VP layers lined along the film pores. The P2VP layers would serve as barriers if the nonpolar solvent has a weak affinity for P2VP although the P2VP layers are very thin with the thickness of a few nanometers.[26] The third step is the enrichment of CH in the PS framework, which leads to swelling of the PS chains. With the continuous uptake of CH, the mobility of the PS chains is significantly enhanced, eventually resulting in the deformation of the originally glassy PS framework holding the structural stability of the film. Driven by the locomotion of the PS chains, the P2VP chains originally lined on the pore wall are forced to migrate inward to prevent the energetically unfavorable contact with CH. The P2VP chains aggregate to form isolated P2VP microdomains embedded by PS chains. Because of the squeezing effect of the swelling PS chains the size of the pores in the film is progressively reduced until completely sealed. As a result, the original porous framework of the S2VP film collapses, forming a dense and nonporous morphology. Such a closing process is confirmed by the characterization of water contact angles. The as-coated S2VP film exhibits a water contact angle of ~86°, which is close to that of a smooth surface of PS homopolymers,[27] implying that the film is predominantly covered by PS chains. After swelling in ethanol the contact angle drops to ~50° and returns to ~88° later when treated in CH for 5 min, suggesting that a large portion of the PS blocks migrates to the surface of the film during this closing procedure. The reversible switch between the nonporous and the nanoporous state of the BCP films by selective swelling using corresponding solvents is schematically shown in Scheme 1.

However, the closing process carried out in CH is too fast to track *ex situ* investigation. Alternatively, we employed *n*PT as the closing agent since it induces a considerably mild closing of the film. When the porous S2VP film is treated in *n*PT at 30 °C, the pore closing still occurs, but the speed significantly slows down. For the immersion duration of 0.5 h or 1 h, the film still possesses a highly porous morphology (Fig. 2a and b), exhibiting no noticeable change compared to the initial morphology of the film before exposure to *n*PT (Fig. 1a). After extending the exposure time to 3 h, the opening extent on the surface declines moderately (Fig. 2c). Further prolonging the exposure time to 5 h, the vast majority of the pores on the surface are closed, leaving only a few of them (Fig. 2d). When the immersion duration extends to 8 h or 12 h, the morphology change appears to be very slow as there is no clear difference for the film subjected to *n*PT immersion for 5 h and 8 h (Fig. 2d *vs.* Fig. 2e) although an immersion duration of 12 h almost eliminates all the pores on the surface (Fig. 2f). There is no obvious change on the surface morphologies upon further lengthening the duration to 15 h, suggesting that the pore closing in *n*PT proceeds at a much slow rate compared to the case in CH, but the film is infinitely close to the complete closing, dense state.

By comparing Fig. 1 and 2, we found that CH exhibits a much stronger capability to induce the pore closing of S2VP films than *n*PT. For instance, the film treated in CH at 22 °C for 30 s displayed a denser surface than that treated in *n*PT at 30 °C for 3 h (Fig. 1d *vs.* Fig. 2c) although the treatment in *n*PT was much longer at higher temperature. Solvent diffusion in glassy

Table 1 The solubility parameters, molar volumes of solvents, and the calculated polymer–solvent interaction parameters involved in this study

Solvent	$\delta_{Solvent}$ ($MPa^{1/2}$)	Molar volume ($cm^3\ mol^{-1}$)	Temperature (°C)	$\chi_{PS-Solvent}$	$\chi_{P2VP-Solvent}$
CH	16.8	108.7	22	0.48	0.98
			30	0.48	0.96
*n*PT	14.5	116.2	30	1.12	2.06

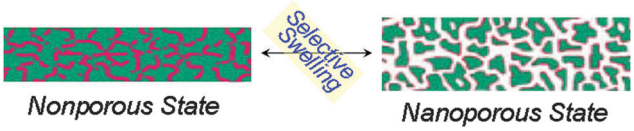

Scheme 1 The schematic of the switching between the nonporous state and the nanoporous state of S2VP films by selective swelling. The PS and P2VP phases are highlighted in green and red color, respectively.

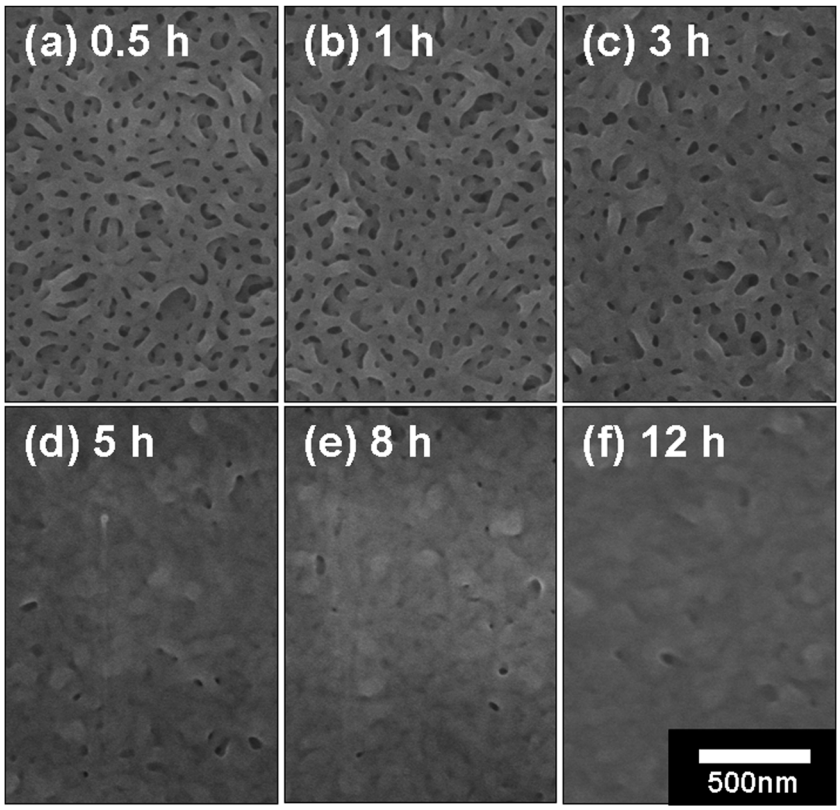

Fig. 2 The surface SEM images of the porous S2VP film exposed to *n*PT at 30 °C for 0.5 h (a), 1 h (b), 3 h (c), 5 h (d), 8 h (e), and 12 h (f). All the SEM images have the same magnification and the scale bar is shown in (f).

polymers is considered to be a case II diffusion with constant solvent penetration velocity, and viscosities as well as molecular sizes of the solvents may influence the diffusion.[28] We note that the viscosity of CH is higher than that of *n*PT (μ_{CH} = 0.980 mPa s and μ_{nPT} = 0.235 mPa s at 25 °C).[29] Moreover, the CH molecule with an estimated size of 4.647 Å × 3.032 Å is slightly bulkier than *n*PT which has a size of 6.890 Å × 1.862 Å. The lower viscosity and the smaller molecular size favor a faster diffusion of *n*PT into the polymer and consequently a stronger pore-closing effect than CH, which is opposite to our observations. Therefore, the slower pore-closing process of *n*PT than CH should only be originated from the difference in their interactions to the copolymer. As can be seen from Table 1, *n*PT exhibits much higher interaction parameters to both PS and P2VP than CH, which means that it has much lower affinity for both blocks. However, χ_{PS-nPT} is smaller than $\chi_{P2VP-nPT}$, suggesting that *n*PT possesses a stronger affinity for PS than P2VP and *n*PT should be considered as a selective solvent to PS. Similar to the exposure of the porous S2VP film to CH, the penetration of *n*PT into the film is also comprised of three steps with a very fast pore filling like in the case of exposure to CH. However, the subsequent P2VP diffusion and PS swelling are significantly retarded as the barrier effect of the P2VP layer becomes more pronounced and it takes a longer duration for PS chains to be swollen to the same extent as a result of a much lower affinity of *n*PT for both P2VP and PS.

The cross-sectional morphologies of these films also reveal a process of progressive pore elimination with the exposure to *n*PT. As clearly shown in Fig. S1 (ESI†), the film became less porous with a continuous reduction in the thickness. We also used ellipsometry to *ex situ* monitor the change of the thickness of the films with different durations of *n*PT exposure. As can be seen from Fig. 3, the thickness drops fast at the initial stage with the exposure duration up to 5 h, and then the reduction of thickness significantly slows down with the extended exposure to *n*PT. For instance, the thickness is drastically reduced from ~1086 nm for the initial film before exposure to *n*PT to ~454 nm after exposure for 5 h, and only slightly reduced to 446, 440, and 430 nm for the exposure duration of 8, 12, and 15 h, respectively. We note that the thickness after exposure for 15 h is very close to the thickness of the initial as-coated nonporous S2VP film before the swelling treatment in ethanol, indicating the complete elimination of pores in the film after exposure to *n*PT for 15 h and the switch to the initial nonporous state of the film. The reduction in thickness proceeds with the progressive uptake of *n*PT. At the initial stage, the driving force for the uptake of *n*PT by PS blocks is large as it is determined by the strong difference in the chemical potential and consequently PS blocks quickly swell, leading to fast reduction in thickness. With the proceeding of *n*PT uptake the difference in the chemical potential diminishes and the PS blocks swell with a continuously reducing rate until saturation. In addition, with the shrinkage of the film pores, the pore filling of the solvent might be nonneglectably hindered in the later stage, which also contributes to the deceleration in the reduction of thickness.

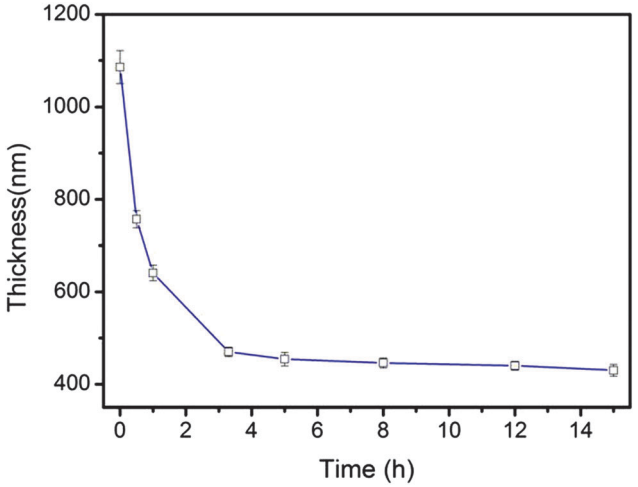

Fig. 3 The thickness of the S2VP film exposed to *n*PT for different durations.

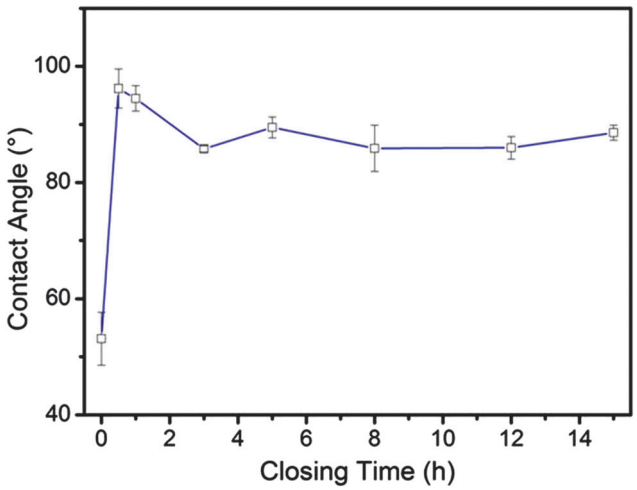

Fig. 4 The water contact angles of the S2VP film exposed to *n*PT for different durations.

Therefore, we observed such an initial fast reduction and a subsequent slow decrease in the thickness of the film exposed to *n*PT. We also investigated the surface composition change of the film exposed to *n*PT for various durations by measuring WCAs. As shown in Fig. 4, the WCA drastically increases to *ca.* 95°, which is close to that of PS homopolymers after exposure of the film to *n*PT for 0.5 h, implying the preferential enrichment of PS chains onto the film surface despite the morphology being unchanged. A slight decrease of WCA from *ca.* 95° to 86° can be detected when the exposure duration prolongs to 1 and 3 h. This may primarily ascribe to the decrease of surface porosity as evidenced by SEM observations, which lowers the WCA as the fraction of air decreases according to Cassie's model.[30] The WCA barely changes with continuous extension of the exposure for more than 3 h as most of the pores on the surface are closed which produces a relatively smooth surface at a swelling duration of 5 h. It is also worth mentioning that the WCA reaches *ca.* 88° after 15 h of exposure to *n*PT, which is almost identical to the WCA of the initial as-coated dense film. Therefore, the surface wettability and the composition of the film can be well-restored in the pore closing procedure by exposure to nonpolar PS-selective solvents.

We also investigated the impact of temperature on the rate of the pore closing as temperature is a key factor in determining the swelling rate.[31] Similar to the pore opening process by ethanol swelling, elevated temperatures require less time to accomplish the pore closure. For example, the pores remained nearly unchanged compared to the initial morphology of the porous film after ethanol swelling when the film was exposed to CH at 22 °C for 10 s (Fig. 1c). In stark contrast, when the temperature slightly increases to 30 °C, exposure to CH for 10 s leads to a complete pore closure, producing a dense film; pores can only be observed at 30 °C for even shorter exposure durations, *e.g.* 5 s (Fig. S2, ESI†). Therefore, the pore closing takes place relatively faster at 30 °C than at 22 °C. This should be mainly attributed to the enhanced mobility of the polymer chains and the diffusion coefficient of the solvent at higher temperatures.[32] In addition, the polymer–solvent parameters will be reduced at elevated temperatures, which increases the affinity of the solvent for both P2VP and PS blocks as suggested by eqn (1). Therefore, a faster diffusion of the solvent into the P2VP chains and a stronger swelling degree of PS blocks can be expected, and eventually the pore closing occurs faster at elevated temperatures.

3.2 Cycling between the pore-open and the pore-closed state

We have demonstrated that the porous S2VP films obtained by selective swelling in ethanol can controllably recover to their initial nonporous, dense morphologies by exposure to nonpolar solvents. Therefore, it becomes very interesting to see whether the film can be repeatedly cycled between the opening and the closing state by exposure to solvents with different selectivities. The cycling between the pore-open and the pore-closed state was carried out by immersing the S2VP film alternatively in ethanol at 70 °C for 1 h and in CH at 30 °C for 5 min. We repeated this pore opening and closing cycles up to 20 times and examined the morphology of the film after exposure to ethanol and to CH for a cycle number of 5, 10, 15, and 20.

As shown in Fig. 5, all the pore-open films (with ethanol exposure as the last treatment) exhibit similar porous morphologies. It is clearly seen that these films possess an interconnected porous structure not only on the surface, but also inside the film as suggested by their cross-sectional morphologies (Fig. S3, ESI†), which is similar to the morphology of the as-coated BCP film subjected to the first exposure to ethanol. However, with the repeat of the cycling process, the surface of the film becomes rougher with the appearance of some breaches. We also investigated the surface as well as cross-sectional morphologies of the pore-closed S2VP films (with the CH exposure as the last treatment) being switched between the two states for different cycles. A dense morphology is observed on these films at different cycles although there are some shallow dents on the film surface, which become more evident at higher cycle numbers. Their dense morphologies are also confirmed by

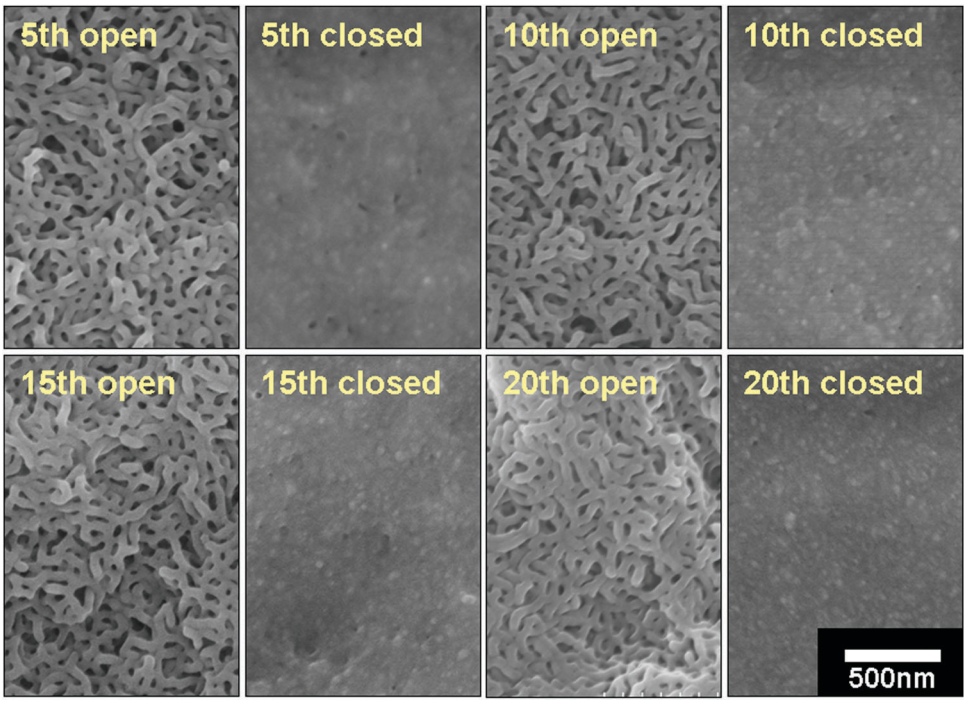

Fig. 5 The surface SEM images of S2VP films in the pore-open and the pore-closed state at different cycle numbers. All the SEM images have the same magnification and the scale bar is shown in the image of the 20th closed state.

the cross-sectional SEM images (Fig. S3, ESI†). Therefore, the BCP films are indeed capable of being reversibly switched between the pore-open state and the pore-closed state at least dozens of times simply by exposure of the film alternatively to solvents selective to different constituent blocks of the copolymer. The appearance of breaches and dents should be due to the relaxation and rearrangement of the polymer chains repeated times.[17]

Moreover, as can be clearly seen from the cross-sectional images of the pore-open films (Fig. S3, ESI†), the thickness of the film being cycled 20 times is evidently larger than that of the film cycled 5 times. To have detailed investigation on the change of the film thickness with cycle times, we measured the thicknesses of films subjected to each exposure to ethanol or CH by ellipsometry and the results are summarized in Fig. 6. First of all, the films in the pore-open state are always two or three folds thicker than those in the pore-closed state in all different cycles. Moreover, the thickness of the pore-open films notably increases with the cycle numbers whereas the films in the pore-closed state experience a very slight increase in thickness with repeated cycles. The thickness of the pore-open film with a cycle number of 5 is ~859 nm and it progressively increases to ~938 nm, ~1151 nm, and ~1325 nm at the cycle number of 10, 15, and 20, respectively. In contrast, the thickness of the pore-closed film only slightly increases from ~435 nm at the cycle number of 5 to ~482 nm at the cycle number of 20. The increase in the thickness of the pore-open films with the cycling times should be originated from the less dense structure of the film after each CH exposure. An exposure to CH at 30 °C for 5 min will eliminate most of the pores in the ethanol-treated films; however, the polymer chains are expected to be packed in a loose state compared to the initial as-coated film as both the PS and P2VP chains cannot be completely recovered to their initial positions in such a short exposure duration. Moreover, there should be a small portion of CH inevitably remaining in the S2VP film after CH exposure followed by a brief drying. These CH molecules are dissolved in the S2VP film, leading to higher free volumes of the film and consequently looser packing of the polymer chains. Loose packing of the polymer chains is confirmed by the slightly increased thickness of the pore-closed films at higher cycle numbers. It should be

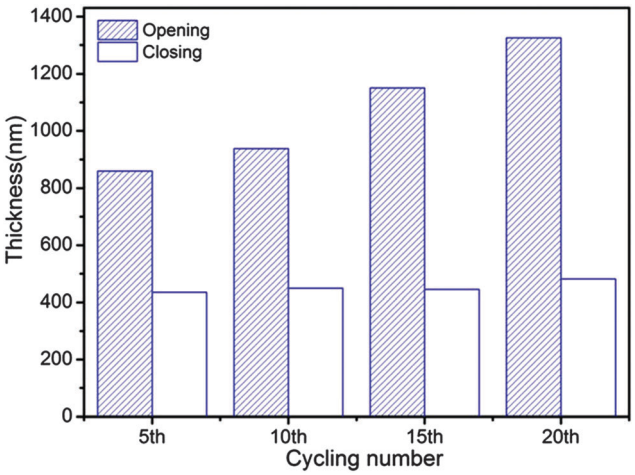

Fig. 6 The thickness of the S2VP films in the pore-open and the pore-closed state at different cycling numbers.

noted that loose packing of polymer chains in the CH-treated S2VP film only leads to higher free volumes, and large pores detectable by SEM do not remain in the film as the CH-treated film is in a complete dense state which can be seen from the cross-sectional SEM images (Fig. S3, ESI†). Upon exposure to ethanol loosely packed polymer chains enhance the penetration of the solvent into the film and the PS and P2VP chains need to move shorter distances to form a P2VP shell/PS core structure, eventually resulting in a porous morphology with a larger porosity and consequently a greater thickness. With increasing exposure times to CH, the film is in an increasingly loose state, and therefore, the film tends to have an even higher porosity and thickness. We note that in these cycling tests each exposure to CH was carried out only for 5 min to avoid a time-consuming and practically unfavourable operation of repeated open and closing cycles. However, it is likely for the loose state of the CH-exposed films to be suppressed to some extent by longer exposure durations, allowing the polymer chains to have sufficient time to return their initial positions.

3.3 Applications of the switchable nanoporous S2VP films in antireflection coatings

The flexible switching between the open and the closed state of the S2VP films readily induced by exposure to correspondingly selective solvents enables their application as intelligent reversible antireflection (AR) coatings in which a controlled porosity resulted from nanopores with sizes smaller than the wavelength of visible light is required. We spincoated the chloroform solution of S2VP with a concentration of 0.8 wt% on cleaned glass slides and obtained a dense S2VP layer with a thickness of 94 nm. The coated slide was then treated in ethanol at 70 °C for 1 h to convert the S2VP layer into the porous state with a thickness of 231 nm as measured by ellipsometry. The ethanol-treated slide was then immersed in CH at 30 °C for 5 min to recover the pore-closed state of the S2VP layer. Such switches between the open and the closed state of the S2VP layer were repeated for multiple cycles by alternative exposure of the slide to ethanol and CH.

Fig. 7a displays the transmittance spectra of the glass slides coated with a S2VP layer in the open state at different cycling numbers. The transmittance of the blank glass varied between 91% and 92% as the wavelength of the incident light ranged from 400 nm to 2000 nm. The transmittance was decreased to 90–91% after spincoating a dense S2VP layer on the slide, which was noticeably increased to 92–94% in the range of wavelengths of ~500–2000 nm after cavitating the dense S2VP layer by exposure to ethanol for the first time. We then exposed the slide to CH to close the pores and observed a transmittance very close to that of the blank slide (Fig. 7b). The second exposure to ethanol cavitated the S2VP layer again and consequently resulted in an enhanced transmittance slightly better than that of the first cavitated ones. Similarly, the second exposure to CH reduced the transmittance but the transmittance was slightly larger than that of the first closed one. We repeatedly exposed the S2VP-coated slides to ethanol and CH up to 10 times and the enhanced and reduced transmittance was permanently observed after exposure to ethanol and CH,

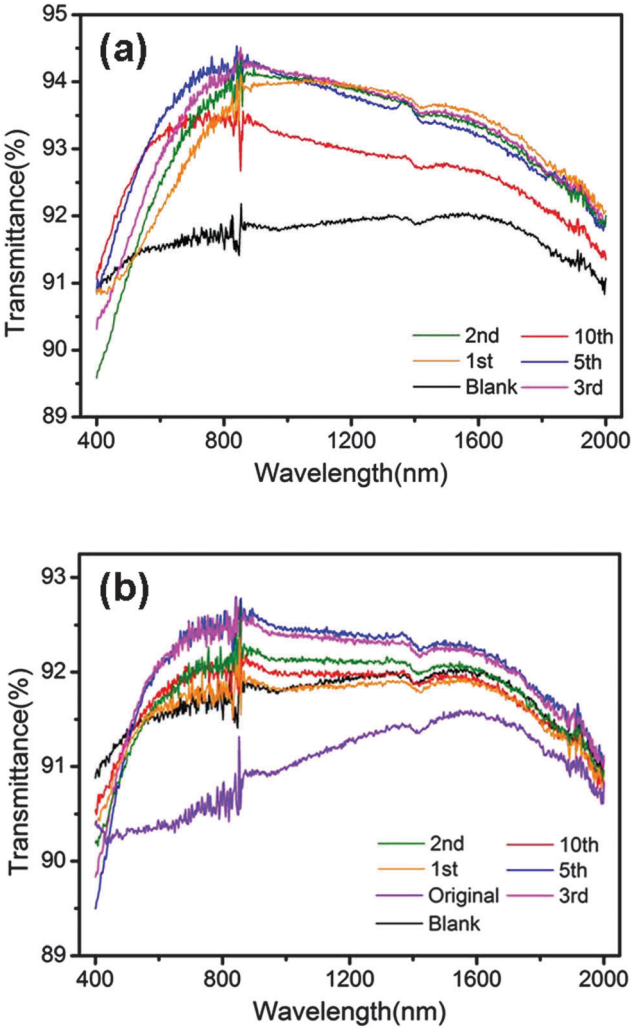

Fig. 7 The transmittance spectra of glass slides with the S2VP coating layer in the pore-open state (a) and in the pore-closed state (b) at different cycling numbers.

respectively. Moreover, with the exposure to ethanol being increased from the first time to the fifth time the maximal transmittance (T_{max}) was continuously increased; however, the slide subjected to the tenth exposure to ethanol was an exception which exhibited a dramatic decrease of transmittance in both visible light and near-infrared (NIR) regions. Interestingly, such a trend was also observed in the CH-exposed slides. With the exposure to CH being increased from the first time to the fifth time, the transmittance remained slightly increased but the tenth exposure to CH led to a decrease in transmittance.

The refractive index of a porous coating layer (n_2) is related to the pristine refractive index of the material in the nonporous state (n_1) as well as the porosity (φ) of this coating layer, which can be calculated using the following equation:[33]

$$n_2^2 = n_1^2(1 - \varphi) + n_0^2\,\varphi \qquad (2)$$

where $n_0 = 1$, representing the refractive index of air. We can see from eqn (2) that n_1 is only determined by the porosity for

coating layers from the same material, and a higher porosity would lead to a lower refractive index.

However, a coating layer with a high porosity or low refractive index does not necessarily promise a high transmittance. For example, the best index of an antireflective layer coated on a glass substrate with a refractive index of 1.52 should be 1.23 to have zero reflectance in air.[31] A coating layer with a refractive index either higher or lower than 1.23 would lead to a portion of reflectance of the incident light and thus 100% transmittance cannot be obtained. The refractive index of the dense S2VP layer is measured to be 1.59 by ellipsometry. After the first immersion in an ethanol bath at 70 °C for 1 h, the porosity of the S2VP layer is estimated to be 59.3% by comparing its thickness before and after ethanol swelling (ESI†), and correspondingly n_2 is estimated to be 1.27 according to eqn (2). As discussed in Section 3.2, the thickness of the pore-open S2VP layer became greater with the times of ethanol exposure (Fig. 6), thus leading to the increase of φ and the reduction of n_2. That is, at the first, second, third, and fifth exposure to ethanol, n_2 kept reducing and was approaching to 1.23, resulting in increased T_{max}. The sudden drop in transmittance for the S2VP layer subjected to the tenth ethanol exposure might be attributed to its extraordinarily high porosity. The presence of the large breaches on the film surface as already observed from the SEM image of the sample (Fig. 5) might also play a role. Such large defects with sizes comparable to the wavelength of incident light result in scattering, thus reducing the light transmittance.[34]

The as-coated dense S2VP layer yields an obvious decline in T_{max}, which is attributed to the higher refractive index of dense S2VP (n = 1.59) than the glass substrate (n = 1.52). The higher transmittance of the pore-closed S2VP layers induced by CH exposure than the original dense S2VP layer should be ascribed to the loose packing of polymer chains, which results in smaller n_1 after exposure to CH at 30 °C for 5 min. Meanwhile, it is noteworthy that T_{max} of the slides with the S2VP layer in the closed state is always lower than those in the open state despite the cycling numbers, which is due to the larger porosity of the latter. Fig. 8 displays the transmittance values at the wavelength of both 600 nm and 1000 nm of the S2VP-coated slide alternatively exposed to ethanol and CH for 10 cycles. The transmittance in both wavelengths corresponding to the visible light region and the NIR region, respectively, fluctuates with the progress of cycling exposure to ethanol and CH. It is apparent that the amplitude in the change of transmittance between the closed and the open state of the S2VP layer at the wavelength of 1000 nm is larger than that at the wavelength of 600 nm. We note that it is flexible and easy to optimize the BCP concentration, the temperature as well as durations of solvent exposure to obtain the required porosity and thickness to fit specific applications. Moreover, S2VP can be coated on both sides of the substrate to obtain even higher transmittance. The reversible switch of the transmittance of the S2VP layers not only provides a potential strategy to prepare intelligent antireflection coatings but also confirms the easy control and switch of the porous nature of the S2VP films simply by alternative exposure to solvents selective to the corresponding blocks of the block copolymer.

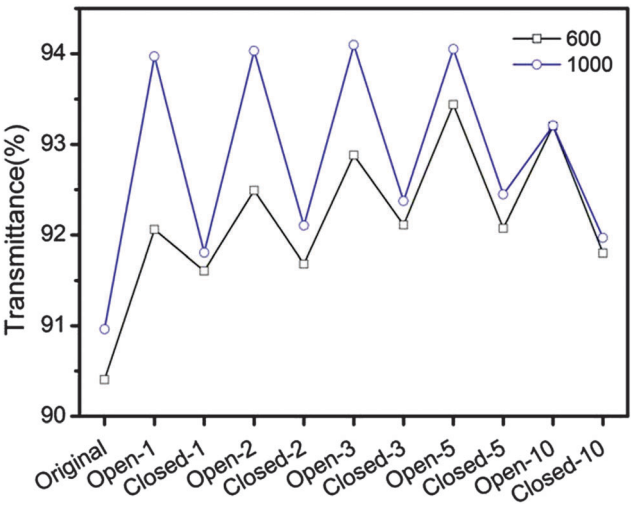

Fig. 8 The transmittance at the wavelength of 600 nm and 1000 nm of a glass slide with the S2VP coating layer in the sequential pore-open and pore-closed state at the first, second, third, fifth, and the tenth cycle.

3.4 Applications of the switchable nanoporous S2VP films in drug delivery

The reversible switch between the nanoporous and the non-porous state of the S2VP films simply by exposure to solvents with different selectivities suggests that they probably are good candidates for drug loading and delivery. The drug loading can be carried out when the film is in the fully pore-open state to accommodate as much drug as possible whereas the drug delivery can be done in the partially closed state to lower the delivery rate. Moreover, the easy control over the closing degree, *i.e.* porosity, of the S2VP films by changing the exposure durations provides a good measure to regulate the delivery rate. We used BSA as the model protein drug and BSA was loaded into the porous S2VP films produced by ethanol swelling at 70 °C for 1 h by the capillary force. The diameter of the BSA molecule is estimated to be 6.8 nm and the pore diameter of the film is over 20 nm,[5] therefore, it should be easy for the BSA molecules to diffuse inside the porous S2VP film under the synergistic effect of the capillary force and the electrostatic interaction between BSA and P2VP blocks enriched on the pore wall. The BSA-loaded S2VP films were then immersed in CH at 30 °C for 30 s or 30 min to close the pores to different degrees. As displayed in Fig. S4 (ESI†), despite the CH exposure durations, the pores largely remain on the film surface, which is in clear contrast to the nearly complete closure of the film without loaded drugs (Fig. 1). This is because the presence of the proteins in the pores resists the recovery of the polymer chains to their initial positions before ethanol swelling. The cross-sectional SEM images reveal that the thickness of the S2VP film subjected to CH exposure for 30 s remains almost unchanged while the morphology is significantly changed to a porous structure composed of stretched fibers from initially a more regular porous structure. An exposure to CH for 30 min greatly reduces the thickness of the S2VP film to 6.4 μm from initially 15 μm and most porosity is lost and the film tends to have a

dense and nonporous morphology. In such a dense structure, the BSA molecules are believed to be tightly entrapped in the S2VP matrix and will not be released without damaging the S2VP matrix. Therefore, we subsequently investigated the release behaviors of the BSA loaded in the S2VP films in PBS solutions at 25 °C with a fully opened state without CH exposure and a partially closed state prepared by exposure to CH for 30 s.

Fig. 9 indicates the cumulative release profiles of BSA from the two S2VP films. Apparently, the fully opened S2VP film without exposure to CH exhibits higher cumulative BSA concentrations in the same release period than the partially opened S2VP film exposed to CH for 30 s, suggesting a larger release rate of the former (Fig. 9a). It can be easily understood that a short exposure to CH partially closes the pores at least in the region near the film surface, thus hindering the diffusion of BSA out from the S2VP film. For further tracking of the long-term release of the S2VP film subjected to CH exposure for 30 s, we observe a generally stable release over the period of 20 days (Fig. 9b).

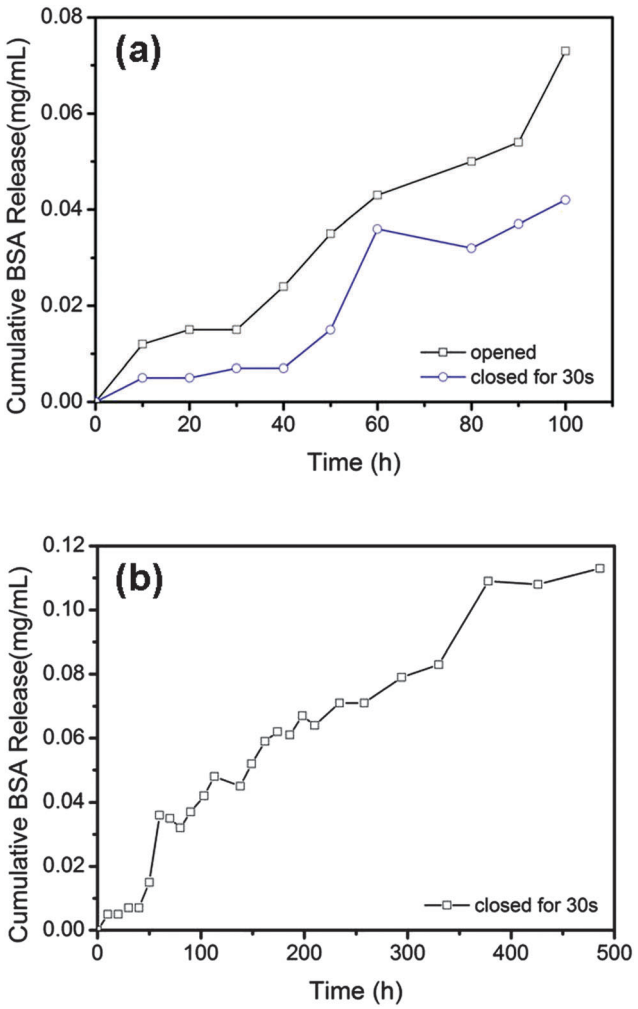

Fig. 9 The cumulative release profiles of BSA from the ethanol-treated S2VP film in the fully pore-open state (without subsequent CH exposure) and the S2VP film in the partially pore-opened state (with a subsequent CH exposure for 30 s) (a) and the long-term release profile of BSA from the latter S2VP film, which is in the partially pore-opened state (b).

Moreover, there is no burst release and the release rate remains generally constant over the investigated 20 days. Such a stable, long-term release should be primarily ascribed to the interconnected porosity with the pore size comparable to the size of the protein of the S2VP films. It should be noted that a strictly linear release of the protein with time from the partially closed film was not yet observed. This is due to that the pores on the surface and also in the interior of the film are not monodispersed and a single-file diffusion of the protein through the film cannot be always guaranteed.[35]

4. Conclusion

S2VP block copolymer films have been demonstrated to repeatedly switch between the nanoporous and the nonporous state simply by alternative exposure of the films to solvents with selectivity towards different blocks. Nanopores are reversibly produced and eliminated by exposure of the film to hot ethanol for hours and to cyclohexane at room temperature for seconds because of the selective swelling of the P2VP microdomains and the PS matrix, respectively. It is found that the exposure duration, temperature, and the interaction parameter between the solvent and the constituent blocks influence the pore-closing process among which the interaction parameter plays the dominated role. Such a switch can be repeated dozens of times and the films in the pore-open state have increased thicknesses with the repeated cycles because of the loose packing of polymer chains. The S2VP films exhibit tunable transmittance in response to the switch between the nanoporous and the nonporous state, implying their potential applications as intelligent antireflection coatings. We also demonstrate that the S2VP films can be used in drug delivery as drugs can be loaded when the films are in the highly porous state whereas drugs can be released in a partially closed state promising a well-regulated slow and stable release rate.

Acknowledgements

Financial support from the National Basic Research Program of China (2015CB655301), the Jiangsu Natural Science Funds for Distinguished Young Scholars (BK2012039), and the Project of Priority Academic Program Development of Jiangsu Higher Education Institutions (PAPD) is gratefully acknowledged.

References

1 J. Hiller, J. D. Mendelsohn and M. F. Rubner, *Nat. Mater.*, 2002, **1**, 59–63.
2 X. Li, X. Yu and Y. Han, *Langmuir*, 2012, **28**, 10584–10591.
3 J. B. Qu, L. Y. Chu, M. Yang, R. Xie, L. Hu and W. M. Chen, *Adv. Funct. Mater.*, 2006, **16**, 1865–1872.
4 K. H. Zhang, X. L. Feng, X. F. Sui, M. A. Hempenius and G. J. Vancso, *Angew. Chem., Int. Ed.*, 2014, **53**, 13789–13793.
5 H. Yu, X. Qiu, S. P. Nunes and K.-V. Peinemann, *Nat. Commun.*, 2014, **5**, 4110.

6 X. Yang, B. A. Moosa, L. Deng, L. Zhao and N. M. Khashab, *Polym. Chem.*, 2011, **2**, 2543–2547.
7 Y. Wang, Z. M. Liu, B. X. Han, Z. X. Dong, J. Q. Wang, D. H. Sun, Y. Huang and G. W. Chen, *Polymer*, 2004, **45**, 855–860.
8 Y. C. Chen, R. Xie and L. Y. Chu, *J. Membr. Sci.*, 2013, **442**, 206–215.
9 X. Y. Qiu, H. Z. Yu, M. Karunakaran, N. Pradeep, S. P. Nunes and K.-V. Peinemann, *ACS Nano*, 2013, **7**, 768–776.
10 J. D. Mendelsohn, C. J. Barrett, V. V. Chan, A. J. Pal, A. M. Mayes and M. F. Rubner, *Langmuir*, 2000, **16**, 5017–5023.
11 A. Fery, B. Scholer, T. Cassagneau and F. Caruso, *Langmuir*, 2001, **17**, 3779–3783.
12 Y. Wang, C. He, W. Xing, F. Li, L. Tong, Z. Chen, X. Liao and M. Steinhart, *Adv. Mater.*, 2010, **22**, 2068–2072.
13 J. Yin, X. Yao, J.-Y. Liou, W. Sun, Y.-S. Sun and Y. Wang, *ACS Nano*, 2013, **7**, 9961–9974.
14 Z. Wang, X. Yao and Y. Wang, *J. Mater. Chem.*, 2012, **22**, 20542–20548.
15 W. Sun, Z. Wang, X. Yao, L. Guo, X. Chen and Y. Wang, *J. Membr. Sci.*, 2014, **466**, 229–237.
16 Z. Chen, C. He, F. Li, L. Tong, X. Liao and Y. Wang, *Langmuir*, 2010, **26**, 8869–8874.
17 D. H. Kim, K. H. A. Lau, W. Joo, J. Peng, U. Jeong, C. J. Hawker, J. K. Kim, T. P. Russell and W. Knoll, *J. Phys. Chem. B*, 2006, **110**, 15381–15388.
18 Y. Wang and F. Li, *Adv. Mater.*, 2011, **23**, 2134–2148.
19 F. Li, X. Yao, Z. Wang, W. Xing, W. Jin, J. Huang and Y. Wang, *Nano Lett.*, 2012, **12**, 5033–5038.
20 H. Fan and Z. Jin, *Macromolecules*, 2014, **47**, 2674–2681.
21 J. Gong, A. Zhang, H. Bai, Q. Zhang, C. Du, L. Li, Y. Hong and J. Li, *Nanoscale*, 2013, **5**, 1195–1204.
22 R. Deng, S. Liu, J. Li, Y. Liao, J. Tao and J. Zhu, *Adv. Mater.*, 2012, **24**, 1889–1893.
23 H. Y. Huang, Z. J. Hu, Y. Z. Chen, F. J. Zhang, Y. M. Gong, T. B. He and C. Wu, *Macromolecules*, 2004, **37**, 6523–6530.
24 H.-C. Kim, S.-M. Park and W. D. Hinsberg, *Chem. Rev.*, 2010, **110**, 146–177.
25 J. Brandrup, E. H. Immergut, E. A. Grulke, A. Abe and D. R. Bloch, *Polymer Handbook*, 4th edn, John Wiley & Sons, New York, 1999.
26 Y. Wang, L. Tong and M. Steinhart, *ACS Nano*, 2011, **5**, 1928–1938.
27 M. L. Wadey, I. F. Hsieh, K. A. Cavicchi and S. Z. D. Cheng, *Macromolecules*, 2012, **45**, 5538–5545.
28 B. A. Miller-Chou and J. L. Koenig, *Macromolecules*, 2003, **36**, 4851–4861.
29 I. M. Smallwood, *Handbook of Organic Solvent Properties*, John Wiley & Sons, New York, 1996.
30 X. J. Feng and L. Jiang, *Adv. Mater.*, 2006, **18**, 3063–3078.
31 J. Yang, L. Tong, Y. Yang, X. Chen, J. Huang, R. Chen and Y. Wang, *J. Mater. Chem. C*, 2013, **1**, 5133–5141.
32 B. Narasimhan and N. A. Peppas, *Macromolecules*, 1996, **29**, 3283–3291.
33 T. C. Choy, *Effective Medium Theory: Principles and Applications*, Oxford University Press, New York, 1999.
34 H. E. Bennett, *Opt. Eng.*, 1978, **17**, 480–488.
35 S. Y. Yang, J. A. Yang, E. S. Kim, G. Jeon, E. J. Oh, K. Y. Choi, S. K. Hahn and J. K. Kim, *ACS Nano*, 2010, **4**, 3817–3822.